Stream function, flow separation and force equation for stagnation flow passing a small solid sphere touching a rising gas bubble

2003 J. Phys. A: Math. Gen. 36 9105

(http://iopscience.iop.org/0305-4470/36/34/311)

INSTITUTE OF PHYSICS PUBLISHING JOURNAL OF PHYSICS A: MATHEMATICAL AND GENERAL

J. Phys. A: Math. Gen. **36** (2003) 9105–9117 PII: S0305-4470(03)63923-5

Stream function, flow separation and force equation for stagnation flow passing a small solid sphere touching a rising gas bubble

Anh V Nguyen and Geoffrey M Evans

Discipline of Chemical Engineering, School of Engineering The University of Newcastle, Callaghan NSW 2308, Australia

E-mail: Anh.Nguyen@newcastle.edu.au

Received 27 May 2003
Published 12 August 2003
Online at stacks.iop.org/JPhysA/36/9105

Abstract

This paper considers an axisymmetric stagnation flow past a small solid sphere touching an air bubble, which is significantly larger than the particle but smaller than the capillary length so that the deformation can be neglected. The disturbed flow due to the presence of the particle at the bubble surface was modelled by considering an axisymmetric stagnation point flow about a sphere and a plane. The stream function for the disturbed flow was derived based on the tangent-sphere coordinates. It is shown that the flow separation having an infinite set of nested ring vortices exists in a finite region enclosing the contact point. The presence of such vortices might have considerable influence on the bubble–particle attachment as well as on the transport of surfactants during the bubble–particle interaction. The force equation was obtained from the derived stream function and was equated to the modified Stokes drag force equation, and then an expression for the correction factor was obtained. The model for the correction factor includes the effect of particle size, and predicts finite force values at zero separation distance between the particle and bubble surfaces. The models presented in this paper should provide a better estimate for calculating the normal (stagnation flow) fluid force acting on particles in contact with bubbles in the multiphase flows found in mineral flotation and other metallurgical operations.

PACS numbers: 47.10.+g, 47.20.−k, 83.50.Lh, 66.29.+d

1. Introduction

The hydrodynamic interaction of fine particles with other surfaces (collection media) is important for a range of industrial processes involving multiphase flows including deep

bed filtration, hindered settling in dewatering thickeners, magnetic separation and flotation separation of particles. In these applications the collection media can be either another solid particle, i.e. filtration media, or an air bubble, as is the case in flotation. In each case, however, the hydrodynamic forces occurring as a result of the particle moving close to collection media surface become significant and cannot be predicted from models developed for the situation when the particles are in the bulk flow.

Previous efforts to include the effect of the hydrodynamic interactions at short separations focused on solid surfaces [1–3] typically encountered, for example, in filtration and hindered settling. The interactions between air bubbles and particles in the flotation separation process [4] represent different situations. The gas–liquid interface in flotation is mobile since during bubble rise the surface-active agents and other impurities are swept to the rear of the bubble by the motion of the water, resulting in the forward bubble surface being mobile and the rear surface being immobile (stagnant cap). Given that a particle usually approaches the front of a bubble, it would be more correct to assume that the bubble has a mobile surface despite the use of different surface-active agents.

It is noted that the mobile liquid–gas interface significantly differs from the solid–liquid interface in the magnitude of the liquid velocity tangential to the interface. In the immobile case the velocity is zero but it is different from zero in the case of the mobile liquid–gas interface. Thus, one can expect that the hydrodynamic interaction between surfaces in the two cases might be different. Unlike solid surfaces, the hydrodynamic interaction at short separations between an air bubble and a solid particle has not attracted much attention despite its significance for the flotation process used in the recovery of minerals and coal from the rock, wastepaper de-inking and wastewater treatment.

The focus of this paper is on the hydrodynamic interaction between an air bubble and a solid spherical particle when the particle touches the gas–liquid interface. The flow field passing the particle is consisted of the shear and axisymmetric stagnation flows in the directions tangential and normal to the bubble surface, respectively (figure 1). The balance of the hydrodynamic force in the normal direction and intermolecular forces between the bubble and the particle determine the particle attachment to the bubble surface. In this paper, we are concerned with the axisymmetric stagnation flow. It is to recall that this paper addresses the initial stage of the bubble–particle attachment interaction where no finite contact angle between a bubble and a particle is made. The subject of a spherical particle straddling a gas–liquid interface relevant to the stability of particle–bubble capture with a contact angle in an extensional flow is studied by Stoos and Leal [5].

2. Mathematical formulation of the problem

2.1. Stream function of the undisturbed axisymmetric stagnation flow

Firstly, it is required to quantify the axisymmetric stagnation flow of the liquid close to the free surface of the bubble in the absence of the particle. This can be determined using the Taylor series expansion [6], giving the following equation for the normal (perpendicular to the bubble surface) velocity component, $\vec{W}$, around the bubble:

$$\vec{W} = \left[W(0) + z\left(\frac{\partial W}{\partial z}\right)_{z=0} + \frac{z^2}{2}\left(\frac{\partial^2 W}{\partial z^2}\right)_{z=0} + \cdots \right]\vec{i}_z = -[2A(z - z^2) + O(z^3)]\vec{i}_z \qquad (2.1)$$

where $\vec{i}$ is the unit vector pointed outwards into the liquid phase (the negative sign indicates liquid flow towards the plane surface), z is the distance measured from the bubble surface and scaled by dividing by the bubble radius, R_b (figure 1) (variables in this paper are

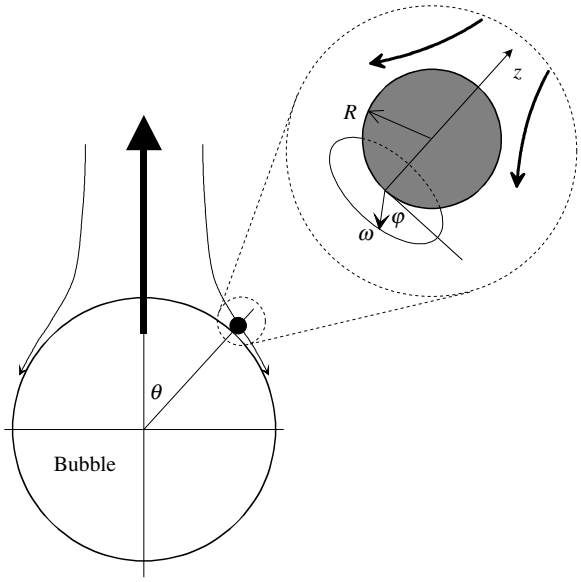

Figure 1. Spherical particle with radius R touching the surface of a rising bubble. The flow field passing the particle is consisted of the shear and axisymmetric stagnation (inset) flows in the directions tangential and normal to the bubble surface, respectively. The local cylindrical coordinate system (ω, φ, z) is used to model the stagnation flow.

non-dimensional and can be obtained from the dimensional ones by appropriate scaling. For instance, velocity and length are scaled by dividing by the bubble rise velocity and the bubble radius, respectively). In equation (2.1), A is given by the functional relationship [6]

$$A = X\cos\theta + \frac{3Y}{2}\cos^2\theta - \frac{Y}{2} \tag{2.2}$$

where θ is the polar angle measured from the front stagnation point, and X and Y are functions of the bubble Reynolds number, $Re = 2\delta R_b U/\mu$, where δ and μ are the liquid density and viscosity, respectively,

$$X = 1 + \frac{0.0637Re}{1 + 0.0438Re^{0.976}} \tag{2.3}$$

$$Y = \frac{0.0537Re}{1 + 0.0318Re^{1.309}}. \tag{2.4}$$

It is important to note that equations (2.2) to (2.4) have been developed from the full numerical results [7] and are valid for the front hemispherical surface (i.e. $0 \leqslant \theta \leqslant \pi/2$) of the rising bubbles only. Consequently, these equations should not be applied in instances where flow field over the entire surface of the bubble is required, for example, drag force determination. This is especially the case when the rear surface of the bubble is likely to be immobile, such as when surfactants or other impurities are present in the liquid.

Using a local cylindrical coordinate system (ω, φ, z), as shown in figure 1, the origin of the system is located at the point where the particle just touches the bubble surface, and the z-axis passes through the centre of the particle, while the ω and φ axes lies on the planar surface. Since there is rotational symmetry about z-axis, only the z- and ω-coordinates are used in the modelling.

Using the local coordinate system, the axial and radial components of the fluid velocity, U, are related to the undisturbed flow stream function, ψ_u, by the following expressions:

$$U_\omega(\omega, z) = \frac{1}{\omega}\frac{\partial \psi_u}{\partial z} \tag{2.5}$$

$$U_z(\omega, z) = -\frac{1}{\omega}\frac{\partial \psi_u}{\partial \omega}. \tag{2.6}$$

Solution of equations (2.5), (2.6), and applying the boundary condition

$$U_z(0, z) = W \tag{2.7}$$

from equation (2.1), yields

$$\psi_u = A(\omega^2 z - \omega^2 z^2). \tag{2.8}$$

2.2. Axisymmetric stagnation flow disturbed by the presence of the particle

The stream function, ψ, for the disturbed flow due to the presence of the particle in contact with the bubble surface, can be related to the stream function for the undisturbed flow by the following expression:

$$\psi = \psi_u + \phi \tag{2.9}$$

where ϕ is the difference between the two stream functions. Clearly, the flow in the presence of the particle is only disturbed locally, so that the stream function ψ at locations far from the particle should be identical to the stream function, ψ_u, of the undisturbed flow. Therefore

$$\phi|_\infty = 0. \tag{2.10}$$

Assuming that the flow over the particle is a creeping flow, then from biharmonic formulation applied to the continuity and the Navier–Stokes equations, it follows that

$$E^2(E^2\phi) = 0. \tag{2.11}$$

The differential operator, E^2, in the reduced cylindrical coordinate system is given by

$$E^2 = \frac{\partial^2}{\partial z^2} - \frac{1}{\omega}\frac{\partial}{\partial \omega} + \frac{\partial^2}{\partial \omega^2}. \tag{2.12}$$

In order to obtain an expression for the disturbed flow stream function, a solution for equation (2.11) needs to be found which satisfies the boundary conditions at the particle and bubble surfaces and also that given by equation (2.10).

3. Method and solution for the disturbed flow field

Before proceeding to find a solution to the stream function for the disturbed flow, it is important to realize that equation (2.11) can be conveniently solved using a transformation of the reduced cylindrical coordinate system into the bispherical coordinate system as first shown in [8, 9]. However, the transformation will lead to a singularity at the point where the particle touches the bubble surface. To overcome this problem the tangent-sphere coordinate systems is used [10].

The new tangent-sphere coordinate system (x, φ, y) is related to the existing cylindrical coordinates (ω, φ, z) by the equations

$$\left(z - \frac{1}{2x}\right)^2 + \omega^2 = \left(\frac{1}{2x}\right)^2 \tag{3.1}$$

$$\left(\omega - \frac{1}{2y}\right)^2 + z^2 = \left(\frac{1}{2y}\right)^2. \tag{3.2}$$

Equations (3.1) and (3.2) have been developed for an axisymmetric system, where the φ coordinate remains unchanged. The numerical factor $1/2$ is introduced to simplify the subsequent conversion relationships between the coordinate systems, i.e.
from cylindrical coordinates to new coordinate system

$$x = \frac{z}{z^2 + \omega^2} \tag{3.3}$$

$$y = \frac{\omega}{z^2 + \omega^2}. \tag{3.4}$$

From new coordinate system to cylindrical coordinates

$$z = \frac{x}{x^2 + y^2} \tag{3.5}$$

$$\omega = \frac{y}{x^2 + y^2}. \tag{3.6}$$

Applying equations (3.5) and (3.6), the stream function for the undisturbed flow, equation (3.8), is given in terms of the new coordinates x and y as follows:

$$\psi_u = \mathrm{A}\left[\frac{xy^2}{(x^2 + y^2)^3} - \frac{x^2y^2}{(x^2 + y^2)^4}\right]. \tag{3.7}$$

Similarly, by applying the chain rule, the differential operator described by equation (2.12) can be described in terms of the new coordinates by

$$E^2 = y(x^2 + y^2)\left[\frac{\partial}{\partial x}\frac{x^2 + y^2}{x}\frac{\partial}{\partial x} + \frac{\partial}{\partial y}\frac{x^2 + y^2}{y}\frac{\partial}{\partial y}\right]. \tag{3.8}$$

The next task is to find a solution for equation (2.11). Applying the separation-of-variable method to solve equation (2.11) in the x–y coordinates, the following expression for ϕ is proposed

$$\phi = (x^2 + y^2)^{-3/2}\sum_{m=0}^{\infty} N_m(x)M_m(y). \tag{3.9}$$

Inserting equation (3.9) into (2.11), and solving using boundary condition described by equation (2.10), gives

$$N_m(x) = (a_m + c_m mx)\cosh(mx) + (b_m + d_m mx)\sinh(mx) \tag{3.10}$$

$$M_m(y) = my J_1(my) \tag{3.11}$$

where J_1 is the Bessel function of the first kind and the first order, and a_m to d_m are unknown parameters, which are independent of x and y.

In order to obtain an expression for the stream function for the disturbed flow, given by equation (2.9) where the undisturbed flow stream function is given by equation (3.7), the unknown parameters a_m to d_m are to be computed. This can be determined employing the boundary conditions applied at the particle and bubble surfaces. However, before proceeding to do this, it is worth noting that in the reduced cylindrical coordinate system a spherical particle touching a bubble surface can be described, in non-dimensional terms, by the expression

$$(z - \kappa)^2 + \omega^2 = \kappa^2 \tag{3.12}$$

where κ is the particle radius made dimensionless by dividing by a characteristic length. In this case the characteristic length is the bubble radius. Equation (3.12) can be equivalently described by $z^2 + \omega^2 = 2\kappa z$. Substitution of this equation into equation (3.3) shows that the particle surface in the transformed tangent-sphere coordinates is described by $x = 1/(2\kappa)$. Therefore, in the modelled (tangent-sphere) coordinates values of constant $x = 1/(2\kappa)$ represent spheres of radius $1/(2x)$, centred at $1/(2x)$, in the physical (cylindrical) coordinates.

As we are primarily concerned with the small particles (with a diameter up to 100 μm), and relatively large bubbles (with a diameter of about 1 mm), the deformation of the gas–liquid interface is insignificant and can be regarded as a planar surface. Therefore, in the physical (cylindrical) coordinates the bubble surface is described by $z = 0$. Inserting $z = 0$ into equation (3.3) gives $x = 0$, which means that the bubble surface in the modelled (tangent-sphere) coordinates is given by x equal to zero. It can be observed that the coordinate transformation changes the bubble–particle geometry by the reverse order, i.e. the geometry of big sphere–small sphere in the physical (cylindrical) coordinates is changed into the geometry of small sphere–big sphere (or the geometry of point-big sphere) in the modelled (tangent-sphere) coordinates. This information can be applied to the particle and bubble surfaces to solve the boundary conditions described below.

At bubble surface

$$x = 0. \tag{3.13}$$

Neglecting stress of the gas inside the bubble, zero normal velocity and zero tangential stress boundary conditions applied to equation (2.9) lead to

$$\phi = -\psi_u \tag{3.14}$$

$$\frac{\partial^2 \phi}{\partial x^2} = -\frac{\partial^2 \psi_u}{\partial x^2}. \tag{3.15}$$

Solving equations (3.14) and (3.15), using equations (3.7) and (3.9)–(3.10), gives

$$a_m = d_m = 0. \tag{3.16}$$

From these equations it can be seen that two of the unknown parameters, a_m and d_m, in equation (3.10) are equal to zero. The remaining two parameters, b_m and c_m, can be computed by considering the particle surface.

At particle surface

$$x = \frac{1}{2\kappa} = \zeta. \tag{3.17}$$

Zero normal and tangential (non-slip) velocity boundary conditions lead to

$$\phi = -\psi_u \tag{3.18}$$

$$\frac{\partial \phi}{\partial x} = -\frac{\partial \psi_u}{\partial x}. \tag{3.19}$$

Solving equations (3.18) and (3.19), using equations (3.9)–(3.11), gives

$$\sum_{m=0}^{\infty} my J_1(my) N_m(\zeta) = -\frac{A\zeta y^2}{(\zeta^2 + y^2)^{3/2}} + \frac{A\zeta^2 y^2}{(\zeta^2 + y^2)^{5/2}} \tag{3.20}$$

$$\sum_{m=0}^{\infty} my J_1(my) N'_m(\zeta) = -\frac{Ay^2}{(\zeta^2 + y^2)^{3/2}} + \frac{A(2\zeta y^2 + 3\zeta^2 y^2)}{(\zeta^2 + y^2)^{5/2}} - \frac{5A\zeta^3 y^2}{(\zeta^2 + y^2)^{7/2}} \tag{3.21}$$

where $N'_m(\zeta)$ describes the first derivative with respect to ζ. Equations (3.20) and (3.21) are to be solved for $N_m(\zeta)$and its derivative. The solution can be obtained by expanding the right-hand sides of the equations into the series of the Bessel function similar to those on the left-hand side. We have the mathematical relationships derived from [11], i.e.

$$\frac{y^2}{(\zeta^2+y^2)^{3/2}} = \sum_{m=0}^{\infty} my J_1(my)\exp(-m\zeta) \tag{3.22}$$

$$\frac{3\zeta y^2}{(\zeta^2+y^2)^{5/2}} = \sum_{m=0}^{\infty} m^2 y J_1(my)\exp(-m\zeta) \tag{3.23}$$

$$\frac{15\zeta^2 y^2}{(\zeta^2+y^2)^{7/2}} = \sum_{m=0}^{\infty} (m^2+m/\zeta) my J_1(my)\exp(-m\zeta). \tag{3.24}$$

Substituting these relationships into equations (3.20) and (3.21) we obtain the following equations:

$$N_m(\zeta) = -A\zeta\left\{1-\frac{m}{3}\right\}\exp(-m\zeta) \tag{3.25}$$

$$\frac{\mathrm{d}N_m(\zeta)}{\mathrm{d}\zeta} = A(m\zeta-1)\left\{1-\frac{m}{3}\right\}\exp(-m\zeta). \tag{3.26}$$

Equating equations (3.25) and (3.10), where $x=\zeta$, and making use of equations (3.16) and (3.26), yield the following results:

$$b_m(\zeta) = -\frac{2A\zeta^2 m[1-m/3]}{\sinh(2\zeta m)-2\zeta m} \tag{3.27}$$

$$c_m(\zeta) = \frac{A[2\zeta m+\exp(-2\zeta m)-1][1-m/3]}{m\sinh(2\zeta m)-2\zeta m^2} \tag{3.28}$$

where b_m and c_m are the remaining unknown parameters used in the stream function for the disturbed flow, i.e.

$$\psi = \psi_u + (x^2+y^2)^{-3/2}\sum_{m=0}^{\infty} my J_1(my)\{b_m(\zeta)\sinh mx + c_m(\zeta)mx\cosh mx\}. \tag{3.29}$$

In this equation ψ_u is the stream function for the undisturbed flow in the new coordinate system and is given by equation (3.7). Substitution of equations (3.7), (3.27) and (3.28) into equation (3.29) gives after rearranging

$$\psi = \frac{Ay}{(x^2+y^2)^{3/2}}\sum_{m=0}^{\infty} f(\zeta,m,x)\frac{mJ_1(my)}{\sinh 2\zeta m-2\zeta m}\left(1-\frac{m}{3}\right) \tag{3.30}$$

where

$$f(\zeta,m,x) = [x\cosh(2\zeta m-xm)-x\cosh mx+2\zeta m(x-\zeta)\sinh mx]. \tag{3.31}$$

Finally, it can be seen that equation (3.30) is not a function of the particle-interface separation distance, thus removing the singularity problem encountered when the particle is in contact with a bubble surface and bispherical coordinate system is used.

The stream functions for both the undisturbed (dashed lines) and disturbed (solid lines) flow have been plotted in figure 2 as a function of the original cylindrical coordinate system. The undisturbed flow stream function was calculated from equation (2.8), while the disturbed

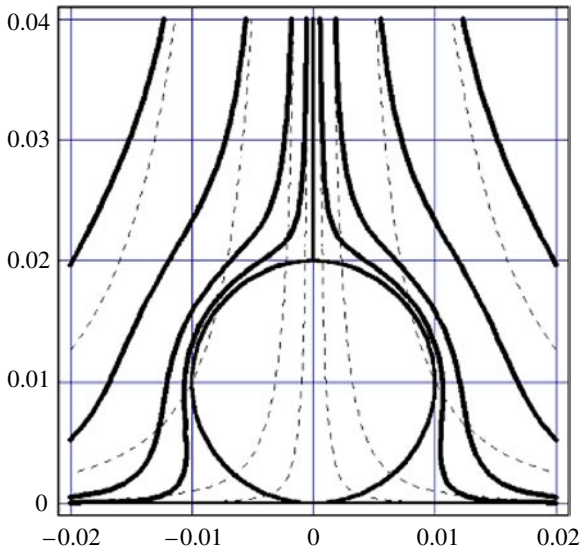

Figure 2. A meridional section of streamlines for the undisturbed (dashed lines) and disturbed (solid lines) flow field. $\kappa = 0.01$; $\psi/A = 10^{-8}, 10^{-7}, 10^{-6}$; $\psi_u/A = 10^{-8}, 10^{-7}, 10^{-6}, 10^{-5}$.

flow stream function was obtained from equation (3.29). Coordinates x and y in equation (3.29) are calculated from the original cylindrical coordinate system using equations (3.3) and (3.4). It can be seen that far from the particle surface the stream functions for both the undisturbed and disturbed flows are similar (the same for infinite distances). However, as expected, the stream functions deviate from each other as the fluid moves closer to the particle surface, to the extent that the undisturbed flow stream functions pass through the particle. For the disturbed flow case, the surface of the particle and bubble is defined by a single stream function originating in the flow upstream of the front stagnation point on the particle surface.

4. Force exerted by the flow on the touching particle

The previous sections have focused on deriving an expression for the stream function, equation (3.30), for the disturbed flow. The stream function can be used to calculate the force acting on a particle with radius, R, as shown in [9, 12], i.e.

$$F = (\pi \eta R/\kappa) \int \omega^3 \frac{\partial}{\partial n} \left(\frac{E^2 \psi}{\omega^2} \right) \mathrm{d}s \tag{4.1}$$

where n and s are the normal and tangential coordinates to the particle surface, and κ has been included in the scaling of the dimensional cylindrical coordinates. Applying the chain rule, both n and s can be transformed into the new coordinate system, such that

$$\frac{\partial}{\partial n} = (x^2 + y^2) \frac{\partial}{\partial x} \tag{4.2}$$

$$\mathrm{d}s = \frac{\mathrm{d}y}{x^2 + y^2}. \tag{4.3}$$

Using these results, and substituting equation (3.30) into (4.1), integration over the particle surface, i.e. at $x = \zeta$ and $0 \leqslant y \leqslant \infty$, and after lengthy algebra yields

$$F = -16\pi\eta A R\kappa \sum_{m=0}^{\infty} \frac{m^3\zeta^4}{\sinh 2m\zeta - 2m\zeta} + \frac{32\pi\mu A R\kappa^2}{3} \sum_{m=0}^{\infty} \frac{m^4\zeta^5}{\sinh 2m\zeta - 2m\zeta} \tag{4.4}$$

and after numerical calculation of the infinite sums leads to

$$F = -16\pi\eta A R\kappa \times 1.529\,03 + \frac{32\pi\eta A R\kappa^2}{3} \times 2.029\,94. \tag{4.5}$$

Equation (4.5) can be used to calculate the force acting on a particle in contact with a mobile planar (bubble) surface in a fluid flow which has a stream function described by the characteristic parameter, A, defined in equation (2.2). It can be equated to the corrected Stokes' drag force equation

$$F = 6\pi\mu R_p W \times f \tag{4.6}$$

to obtain an expression for the correction factor, f, associated with the motion of the fluid. Equating equations (4.5) and (4.6) gives

$$f = -\frac{2A}{W}(2.039\kappa - 1.804\kappa^2). \tag{4.7}$$

Note that W in this equation is to be calculated at the particle centre. Substituting the relationship between A and W, derived from equation (2.2), where z is equal to κ, leads to

$$f = \frac{2.039 - 1.804\kappa}{1 - \kappa}. \tag{4.8}$$

In the limit $\kappa = 0$, equation (4.8) predicts $f = 2.039$. This value is close to 2.034, which is often cited in the literature [6, 7] for the situations where particles are in close contact with bubbles in mineral flotation applications. In this situation, the ratio of the particle to the bubble ratio often exceeds 0.1, i.e. $\kappa > 0.1$, and it would be beneficial to use the expression for the correction factor, f, described by equation (4.8).

In real flotation systems, the bubble–particle interaction is influenced by the presence of other bubbles and particles. In this case, the velocity of the liquid flow disturbed by the bubble is strongly affected by, for example, the finite volume fraction of dispersed bubbles (known as the gas holdup). Therefore, the model parameters X and Y described by equations (2.3), (2.4) are functions of the gas holdup [7]. The effect of the gas holdup on the liquid resistance on the particle can be accounted for using equation (4.6), where velocity W is also a function of the gas holdup, which can be predicted using equations (2.1) and (2.2). The modelling of the gas holdup effect on the correction factor f can be done by changing the infinite boundary condition given by equation (2.10) to finite boundary, which is a difficult analytical task and is beyond the scope of this paper.

Moreover, in the actual flotation process bubble surfaces are neither completely mobile nor completely immobile, but between in these extreme cases. Even if the leading surface of bubbles, where the bubble–particle attachment likely occurs is clean, there are surfactants accumulated on the rear of the bubble surface, which influence the liquid flow passing the bubble. The results obtained in this paper will need to be extended to these cases in a forthcoming paper.

5. Flow separation around the point of contact

It should be mentioned that the streamlines shown in figure 2 were obtained with the Mathematica^{TM} program. A limitation with the analysis was that equation (3.30) did not

produce any streamlines in the area enclosed between the surfaces around the contact point. Detailed analysis revealed that this was caused by the flow separation similar to the Moffatt eddies and vortices that exist in the 2D flow near a sharp corner between two intersecting planes [13].

To model the flow separation the infinite sum in equation (3.30) was replaced by an integral, i.e.

$$\psi = \frac{Ay}{(x^2+y^2)^{3/2}} \left\{ \int_0^\infty \frac{f(\zeta,m,x)J_1(my)}{\sinh 2\zeta m - 2\zeta m}\,\mathrm{d}m - \frac{1}{3}\int_0^\infty \frac{f(\zeta,m,x)mJ_1(my)}{\sinh 2\zeta m - 2\zeta m}\,\mathrm{d}m \right\} \tag{5.1}$$

where m was allowed to be a complex number. The integrals in equation (5.1) were evaluated using a contour integration.

Given that the integrand of the first integral of equation (5.1) is an even function of m, the term can be written as

$$\int_0^\infty \frac{f(\zeta,m,x)J_1(my)}{\sinh 2\zeta m - 2\zeta m}\,\mathrm{d}m = \frac{1}{2}\int_{-\infty}^\infty \frac{f(\zeta,m,x)J_1(my)}{\sinh 2\zeta m - 2\zeta m}\,\mathrm{d}m. \tag{5.2}$$

Using the identity

$$\frac{\mathrm{d}}{\mathrm{d}y}J_0(my) = -mJ_1(my) \tag{5.3}$$

for the derivatives of Bessel functions, J_0 and J_1, of the first kind and zero and first order, respectively, it can be shown that equation (5.2) gives

$$\int_0^\infty \frac{f(\zeta,m,x)J_1(my)}{\sinh 2\zeta m - 2\zeta m}\,\mathrm{d}m = -\frac{1}{2}\frac{\mathrm{d}}{\mathrm{d}y}\int_{-\infty}^\infty \frac{f(\zeta,m,x)J_0(my)}{m(\sinh 2\zeta m - 2\zeta m)}\,\mathrm{d}m. \tag{5.4}$$

Similarly, the second integral of equation (5.1) gives

$$\int_0^\infty \frac{f(\zeta,m,x)mJ_1(my)}{\sinh 2\zeta m - 2\zeta m}\,\mathrm{d}m = -\frac{\mathrm{d}}{\mathrm{d}y}\int_0^\infty \frac{f(\zeta,m,x)J_0(my)}{\sinh 2\zeta m - 2\zeta m}\,\mathrm{d}m. \tag{5.5}$$

The integrand on the right-hand side of equation (5.5) is now an even function of m, and can therefore be rewritten as

$$\int_0^\infty \frac{f(\zeta,m,x)mJ_1(my)}{\sinh 2\zeta m - 2\zeta m}\,\mathrm{d}m = -\frac{1}{2}\frac{\mathrm{d}}{\mathrm{d}y}\int_{-\infty}^\infty \frac{f(\zeta,m,x)J_0(my)}{\sinh 2\zeta m - 2\zeta m}\,\mathrm{d}m. \tag{5.6}$$

Inserting equations (5.4) and (5.6) into equation (5.1) gives

$$\psi = \frac{-Ay/2}{(x^2+y^2)^{3/2}}\frac{\mathrm{d}}{\mathrm{d}y}\left\{ \int_{-\infty}^\infty \frac{f(\zeta,m,x)J_0(my)}{\sinh 2\zeta m - 2\zeta m}\left(\frac{1}{m}-\frac{1}{3}\right)\mathrm{d}m \right\}. \tag{5.7}$$

The next step is to describe the Bessel function J_0 as a contour integral, i.e.

$$J_0(my) = -\frac{2\mathrm{i}}{\pi}\int_1^\infty (t^2-1)^{-1/2}\exp(\mathrm{i}myt)\,\mathrm{d}t \tag{5.8}$$

where $\mathrm{i} = \sqrt{-1}$ and t is a parameter. Equation (5.7) can further be rearranged to give

$$\psi = \frac{\mathrm{i}Ay}{\pi(x^2+y^2)^{3/2}}\frac{\mathrm{d}}{\mathrm{d}y}\left\{ \int_1^\infty \frac{\mathrm{d}t}{\sqrt{t^2-1}}\left[\int_{-\infty}^\infty \frac{f(\zeta,m,x)\,\mathrm{e}^{\mathrm{i}myt}}{\sinh 2\zeta m - 2\zeta m}\left(\frac{1}{m}-\frac{1}{3}\right)\mathrm{d}m \right] \right\}. \tag{5.9}$$

The m-integral in equation (5.9) can be determined employing the contour integration in the complex m plane. The residue theorem [14] gives

$$\int_{-\infty}^\infty \frac{f(\zeta,m,x)\,\mathrm{e}^{\mathrm{i}myt}}{\sinh 2\zeta m - 2\zeta m}\left(\frac{1}{m}-\frac{1}{3}\right)\mathrm{d}m = 2\pi\mathrm{i}\sum_{n=1}^\infty \frac{f(\zeta,m_n,x)\,\mathrm{e}^{\mathrm{i}m_nyt}}{\zeta(\cosh 2\zeta m_n - 1)}\left(\frac{1}{m_n}-\frac{1}{3}\right) \tag{5.10}$$

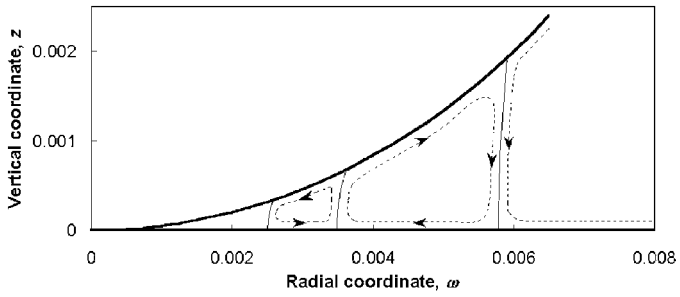

Figure 3. A meridional section of the separation stream surfaces $\psi = 0$ attached to the surfaces and the nested ring vortices around the contact. $\kappa = 0.01$.

Table 1. The first few solutions to equation (5.11) in the first quadrant for the poles of the contour integration.

N	Real part, Re$(2\zeta m_n)$	Imaginary part, Im$(2\zeta m_n)$
1	2.768 678	7.497 676
2	3.352 210	13.899 96
3	3.716 768	20.238 52
4	3.983 142	26.554 55
5	4.193 251	32.859 74
6	4.366 795	39.158 82

where m_n is a pole of the contour integration and can be obtained from the equation

$$\sinh 2\zeta m_n = 2\zeta m_n. \tag{5.11}$$

Substituting equation (5.10) into (5.9) and carrying out the t-integration followed by the y-derivative give

$$\psi = \frac{-2Ay}{\zeta(x^2+y^2)^{3/2}} \operatorname{Im}\left\{\sum_{n=1}^{\infty} \frac{f(\zeta, m_n, x)}{\cosh 2\zeta m_n - 1}\left[1 - \frac{m_n}{3}\right] K_1(-\mathrm{i}m_n y)\right\} \tag{5.12}$$

where Im$\{z\}$ describes the imaginary part of the complex number z, and K_1 is the modified Bessel function of the second kind and first order.

The pole, m_n, of the contour integration must be known for the calculation of the stream function described by equation (5.12). The first few numerical solutions to equation (5.11) for the poles in the first quadrant are given in terms of $2\zeta m_n$ in table 1. Clearly, $-m_n$ and the complex conjugate, $\pm\bar{m}_n$, are also the solutions for the poles.

The calculation of the stream function given by equation (5.12) indicates that there exists an infinite set of stream surfaces on which $\psi = 0$. These surfaces bound an infinite set of nested ring vortices with axes along the z-axis, and are attached to the gas–liquid and particle surfaces as can be seen from figure 3. The locations of the attachment of the stream surfaces $\psi = 0$ can be determined from the conditions of flow separation, which gives

$$\left(\frac{\partial \psi}{\partial x}\right)_{x=0} = 0 \tag{5.13}$$

$$\left(\frac{\partial^2 \psi}{\partial x^2}\right)_{x=\zeta} = 0. \tag{5.14}$$

Table 2. Coordinates of the attachment points of the stream surfaces $\psi = 0$ to the gas–liquid and particle surface with a scaled radius $\kappa = 0.01$.

	Attachment to gas–liquid interface			Attachment to particle surface		
l	Y	ω	z	y	ω	z
1	172.939	0.005 78	0	153.048	0.005 90	0.001 93
2	286.530	0.003 62	0	266.665	0.003 62	0.000 679
3	400.054	0.002 46	0	380.194	0.002 58	0.000 340

Substitution of equation (5.12) into equations (5.13) and (5.14) gives

$$\mathrm{Im}\left\{\sum_{n=1}^{\infty}(1-\cosh 2\zeta m_n)\left(1-\frac{m_n}{3}\right)K_1(-\mathrm{i}m_n y)\right\}=0 \qquad \text{at} \quad x=0 \tag{5.15}$$

$$\mathrm{Im}\left\{\sum_{n=1}^{\infty}\sinh\zeta m_n\left(m_n-\frac{m_n^2}{3}\right)K_1(-\mathrm{i}m_n y)\right\}=0 \qquad \text{at} \quad x=\zeta \tag{5.16}$$

for the criterion equations for determining the coordinate, y, of the attachment of the stream surfaces $\psi = 0$ to the gas–liquid and particle surface, respectively. These equations can be solved to give

$$\arg\left\{\sum_{n=1}^{\infty}(1-\cosh 2\zeta m_n)\left(1-\frac{m_n}{3}\right)K_1(-\mathrm{i}m_n y)\right\}=l\pi \qquad \text{at} \quad x=0 \tag{5.17}$$

$$\arg\left\{\sum_{n=1}^{\infty}\sinh\zeta m_n\left(m_n-\frac{m_n^2}{3}\right)K_1(-\mathrm{i}m_n y)\right\}=l\pi \qquad \text{at} \quad x=\zeta \tag{5.18}$$

where l is an integer and $\arg\{z\}$ describes the argument of the complex number z. The numerical solutions to equations (5.17) and (5.18) converge very fast with increasing the summation index n. Typical results are shown in table 2.

The flow separation shown in figure 3 is similar in profile to the Moffatt vortices reported for confined flows between solid surfaces with no-slip boundaries [15, 16]. In the case of a solid particle in contact with a slip gas–liquid interface, as considered in this study, the flow separation region is smaller. Similarly, it is reported [17] that the flow separation region of unconfined flows on the surface of single bubbles (with slip boundary) is smaller than on the surface of single solid particles (with no-slip boundary), to the extent that at sufficiently low Reynolds numbers no separation occurs on the bubble surface at all.

Although not shown in this paper, the observed flow separation in the region around the bubble–particle contact will have significant influence on the thinning and rupture of the intervening liquid film during the bubble–particle attachment as well as on the mass transfer of surface-active reagents during the bubble–particle interaction with a moving three-phase gas–solid–liquid contact.

6. Conclusions

This paper is concerned with the problem of liquid flow over a fine solid sphere with no-slip boundary touching an air bubble with slip boundary. The bubble considered was larger than the particle but significantly smaller than the capillary length (2.7 mm) so that the deformation

could be safely neglected. The local particle–bubble geometry was physically approximated to the sphere-plane geometry, and the sphere-tangent coordinate system was used to solve the Navier–Stokes equations for creeping flow.

Based on the tangent-sphere coordinates the stream function for the disturbed flow was derived. The force equation of the liquid flow on the particle was obtained by integrating the stream function for the disturbed flow over the particle surface, and then equated to the modified Stokes drag force equation to obtain an expression for the correction factor. The model for the correction factor includes the effect of particle size, and predicts finite force values at zero separation distance.

It was further shown that there exists flow separation region enclosing the contact point having an infinite set of nested ring vortices. The presence of such vortices is likely to have considerable influence on the bubble–particle attachment as well as on the transport of surfactants during the bubble–particle interaction.

Acknowledgments

The authors gratefully acknowledge the Australian Research Council and the Research Management Committee of the University of Newcastle for financial support.

References

[1] Goren S L and O'Neill M E 1971 *Chem. Eng. Sci.* **26** 325–38
[2] Fitzpatrick J A and Spielman L A 1973 *J. Colloid Interface Sci.* **43** 350–69
[3] Malysa K and Van de Ven T G M 1986 *Int. J. Multiph. Flow* **12** 459–68
[4] Leja J 1982 *Surface Chemistry of Froth Flotation* (New York: Plenum)
[5] Stoos J A and Leal L G 1990 *J. Fluid Mech.* **217** 263–98
[6] Nguyen A V 1998 *Int. J. Miner. Process.* **55** 73–86
[7] Nguyen A V 1999 *Int. J. Miner. Process.* **56** 165–205
[8] Stimson M and Jeffery G B 1926 *Proc. Roy. Soc.* A **111** 110–26
[9] Happel J and Brenner H 1965 *Low Reynolds Number Hydrodynamics* (Englewood Cliffs, NJ: Prentice-Hall)
[10] Davis A M J, O'Neill M E, Dorrepaal J M and Ranger K B 1976 *J. Fluid Mech.* **77** 625–44
[11] Magnus W, Oberhettinger F and Soni R P 1966 *Formulas and Theorem for Special Functions of Mathematical Physics* (New York: Springer)
[12] Kim S and Karrila S J 1991 *Microhydrodynamics: Principles and Selected Applications* (Boston, MA: Butterworth-Heinemann)
[13] Moffatt H K 1964 *J. Fluid Mech.* **18** 1–12
[14] Morse P M and Feshbach H 1953 *Methods of Theoretical Physics* (New York: McGraw-Hill)
[15] Schubert G 1967 *J. Fluid Mech.* **27** 647–51
[16] Davis A M J and O'Neill M E 1977 *Chem. Eng. Sci.* **32** 899–906
[17] Clift R, Grace J R and Weber M E 1978 *Bubbles, Drops and Particles* (New York: Academic)